1	Running title:	hispolon induces	human hepatoma	cell apoptosis
---	----------------	------------------	----------------	----------------

# Hispolon Induces Apoptosis and Cell Cycle Arrest of Human Hepatocellular Carcinoma Hep3B Cells by Modulating ERK Phosphorylation

# 5

6 Guan-Jhong Huang<sup>\*†</sup>, Jeng-Shyan Deng<sup> $\nabla$ </sup>, Shyh-Shyun Huang<sup>†</sup>, and Miao-Lin Hu<sup>\*‡§</sup>

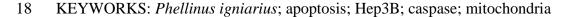
7

- 8 <sup>†</sup> School of Chinese Pharmaceutical Sciences and Chinese Medicine Resources, College of Pharmacy,
- 9 China Medical University, Taichung, Taiwan;
- 10 <sup>v</sup> Department of Health and Nutrition Biotechnology, Asia University, Taichung 413, Taiwan
- <sup>11</sup> <sup>‡</sup>Department of Food Science and Biotechnology, National Chung Hsing University, Kuo-Kuang
- 12 Road, Taichung, Taiwan
- 13 <sup>§</sup>Institute of Nutrition, China Medical University, Taichung, Taiwan
- 14
- 15 \*Corresponding author:
- Miao-Lin Hu, Ph.D., Department of Food Science and Biotechnology, National Chung Hsing
   University, 250 Kuo-Kuang Road, Taichung 402, Taiwan

- 18 Tel.: +886 4 2281 2363; Fax: +886 4 2287 6211
- 19 E-mail address: mlhuhu@dragon.nchu.edu.tw
- 20
- 21
- 22
- 23

#### 1 ABSTRACT

2 Hispolon is an active phenolic compound of *Phellinus igniarius*, a mushroom that has recently 3 been shown to have antioxidant, anti-inflammatory, and anticancer activities. In this study, we investigated the antiproliferative effect of hispolon on human hepatocellular carcinoma Hep3B cells 4 5 by using the MTT assay, DNA fragmentation, DAPI (40, 6-diamidino-2-phenylindole dihydrochloride) staining and flow cytometric analyses. Hispolon inhibited cellular growth of Hep3B 6 7 cells in a time-dependent and dose-dependent manner, through the induction of cell cycle arrest at S 8 phase measured using flow cytometric analysis and apoptotic cell death, as demonstrated by DNA 9 laddering. Hispolon-induced S-phase arrest was associated with a marked decrease in the protein 10 expression of cyclins A, and E and cyclin-dependent kinases (CDKs) 2, with concomitant induction 11 of p21waf1/Cip1 and p27Kip1. Exposure of Hep3B cells to Hispolon resulted in apoptosis as 12 evidenced by caspase activation, PARP cleavage, and DNA fragmentation. Hispolon treatment also 13 activated JNK, p38 MAPK and ERK expression. Inhibitors of ERK (PB98095), but not those of JNK (SP600125) and p38 MAPK (SB203580), suppressed hispolon-induced S-phase arrest and apoptosis 14 15 in Hep3B cells. These findings establish a mechanistic link between MAPK pathway, and 16 hispolon-induced cell cycle arrest and apoptosis in Hep3B cells.



## 19 **INTRODUCTION**

20 Hepatocellular carcinoma (HCC) is a lethal and one of the four most prevalent 21 malignancies in adults in Taiwan, China, and Korea. Several etiologic factors, 22 including exposure to aflatoxin B1, and infection with hepatitis B virus and hepatitis 23 C virus, have been classified as high-risk factors associated with HCC (1). Apoptosis is important in the control of cell quantity during development and proliferation. The 24 25 mechanism of apoptosis is conserved from lower eukaryotes to mammals and exhibits 26 a network of tightly ordered molecular events that finally converge into the enzymatic 27 fragmentation of chromosomal DNA, driving a cell to death (2). Apoptosis involves 28 the activation of a family of caspases, which cleave a variety of cellular substrates that 29 contribute to detrimental biochemical and morphological changes (3). At least two 30 pathways of caspase activation for apoptosis induction have been characterized. One 31 is mediated by the death receptor, Fas. Activation of Fas by binding with its natural 32 ligand (Fas ligand) induces apoptosis in sensitive cells (4). Fas ligand characteristically initiates signaling via receptor oligomerization and recruitment of 33 34 specialized adaptor proteins followed by proteolysis and activation of procaspase-8. 35 Caspase-8 directly cleaves and activates caspase-3, which in turn cleaves other 36 caspases (e.g., caspase-6 and -7) for activation (5). The other pathway, driven by Bcl-2 37 family proteins, which may be anti-apoptotic (Bcl-2 and Bcl-X<sub>I</sub>) or pro-apoptotic

38	(Bax, Bak, and Bid), regulates cell death by controlling the permeability of
39	mitochondrial membrane during apoptosis (6). Upon apoptosis, pro-apoptotic proteins
40	translocate to the mitochondria and accelerate the opening of mitochondrial porin
41	channels, leading to release of cytochrome $c$ and thereby triggering the cascade of
42	caspase activation (7). The induction of apoptosis by natural products on malignant
43	cells validates a promising strategy for human cancer chemoprevention (8).
44	Phellinus linteus (Berk. & M.A. Curt.) (PL) is a mushroom that belongs to the
45	genus Phellinus and is commonly called "Sangwhang" in Taiwan. It is popular in
46	oriental countries and has been traditionally used as food and medicine. PL contains
47	many bioactive compounds, and is known to improve health and to prevent and
48	remedy various diseases, such as gastroenteric disorders, lymphatic diseases, and
49	cancer (9). Recently, a few pharmacological actions of PL have been elucidated. For
50	instance, PL suppresses cellular proliferation and it induces apoptosis in lung and
51	prostate cancer cells (10). The anticancer effects of PL have been demonstrated by the
52	inhibition of invasive melanoma B16-BL6 cells (11). PL has been found to inhibit the
53	growth, angiogenesis and invasive behavior of breast cancer cells via the suppression
54	of AKT phosphorylation (12). We recently reported that hispolon, a phenol compound
55	isolated from PL, anti-inflammatory (13) and antimetastatic effects (14). Others have
56	also shown that hispolon has antiproliferative and immunomodulatory activities (15).

57 However, there have been no reports on the antiproliferative effects of hispolon in 58 liver cancer cells. In this study, we investigated the anticancer effects of hispolon on 59 three different hepatoma cell lines, including J5, HepG2, and Hep3B cells. A major 60 difference of these three hepatoma cell lines lies in their invasive activities, i.e., J5 >HepG2 =Hep3B, based on their expression levels of thyroid hormone b1 nuclear 61 62 receptor and nm23-H1 (16); the latter is a tumor metastatic suppressor gene that has 63 been identified in murine and human cancer lines (17-19). The purpose of this study 64 was to investigate the anticancer effect of hispolon and to provide scientific rationales 65 for using hispolon as chemopreventive and/or chemotherapeutic agents against liver 66 cancer.

67

#### 68 MATERIALS AND METHODS

69 Chemicals. Dulbecco's modified Eagle's medium (DMEM), 3-(4, 70 5-dimethylthiazolyl-2)-2, 5-diphenyltetrazolium bromide (MTT), and other chemicals 71 were obtained from Sigma Chemical Co. (St. Louis, MO, USA). Trypsin-EDTA, fetal 72 bovine serum (FBS) and penicillin/streptomycin were from Gibco Life Technologies, 73 Inc. (Paisley, UK). Cell culture supplies were purchased from Costar (Corning, Inc., 74 Cypress, CA, USA). The antibody against Bax, Bcl-2, Fas, FasL, Bid, caspase 3,

75	caspase 8, caspase 9, MAPK/extracellular signal-regulated kinase (ERK) 1/2, c-Jun
76	NH <sub>2</sub> -terminal kinase (JNK)/stress-activated protein kinase, and p38 MAPK proteins
77	and phosphorylated proteins were purchased from Cell Signaling Technology
78	(Beverly, MA). Anti-cyclin A, anti-cyclin E, anti-CDK 2, anti-p27, anti-p21, and
79	anti-PARP mouse monoclonal antibody and horseradish peroxidase-conjugated goat
80	anti-mouse IgG antibody were purchased from Santa Cruz Biotechnology Co. (Santa
81	Cruz, CA).

83 Isolation and Characterization of hispolon from Fruiting Body of PL. The fruiting 84 body of PL (about 1.0 kg, air dry weight) was powdered, and extracted with 95% 85 EtOH 6 L at room temperature (3 times, 72h each). Extracts were filtered and 86 combined together, and then evaporated at 40 °C (N-11, Eyela, Japan) to dryness 87 under reduced pressure to give a dark brown residue (40 g). The yield obtained for PL 88 is about 4 %. The crude extract was suspended in H<sub>2</sub>O (1 L), and then partitioned with 89 1 L *n*-hexane ( $\times$  2), 1 L EtOAc ( $\times$  2) and 1 L *n*-butanol ( $\times$  2), successively. Hispolon (Fig.1A) was purified from the EtOAc soluble portion (8 g) by a 90 91 bioassay-guid separation. A portion of the active EtOAc fraction was subjected to

- 92 silica gel chromatography using stepwise CHCl<sub>3</sub>-MeOH (9:1, 8:2, 1:1 v/v) as eluent.
- 93 Final purification was achieved by preparative HPLC (Spherisorb ODS-2 RP18, 5 μm

94	(Promochem), 250×25 mm, acetonitrie-H <sub>2</sub> O (83: 17 v/v), at a flow rate of 10 mL/min
95	and UV detection at 375nm). The identification of hispolon was performed by
96	comparing their physical spectral data with literature values (20).
97	
98	Cell Culture. The hepatocarcinoma J5, HepG2, and Hep3B cell was purchased from
99	the Bioresources Collection and Research Center (BCRC) of the Food Industry
100	Research and Development Institute (Hsinchu, Taiwan). Cells were cultured in plastic
101	dishes containing Dulbecco's Modified Eagle Medium (DMEM) supplemented with
102	10% fetal bovine serum (FBS) in a $CO_2$ incubator (5% $CO_2$ in air) at 37 °C and
103	subcultured every 2 days at a dilution of 1:5 using 0.05% trypsin-0.02% EDTA in
104	Ca <sup>2+</sup> -, Mg <sup>2+</sup> - free phosphate-buffered saline (DPBS).

Assay of Cell Viability. The cells  $(2 \times 10^5)$  were cultured in 96-well plate containing DMEM supplemented with 10% FBS for 1 day to become nearly confluent. Then cells were cultured with hispolon for 24, 48, and 72 h. Then, the cells were washed twice with DPBS and incubated with 100 µL of 0.5 mg/mL MTT for 2 h at 37°C testing for cell viability. The medium was then discarded and 100 µL dimethylsulfoxide (DMSO) was added. After 30-min incubation, absorbance at 570 112 nm was read by a microplate reader. At least three repeats were done for each sample 113 to determine cell proliferation. Decolorization was plotted against the concentration of 114 the sample extracts, and the amount of test sample necessary to decrease 50% 115 absorbance of MTT ( $IC_{50}$ ) was calculated.

116

Assay of DNA Fragmentation. Apoptosis was determined by the presence of 117 118 internucleosomal DNA fragmentation (DNA laddering) after cell treated with 119 increasing dose of hispolon for 48 h, or treated with 45 µM for 24, 48, and 72 h. Hep 3B cells were cultured in 24-well microtiter plates at a density of 2 x  $10^6$  cells/well (1 120 121 mL final volume). To extract genomic DNA, cells were harvested, washed with cold 122 10 mM Tris-HCl, pH 7.5, 100 mM NaCl, 2 mM EDTA, and lysed by adding 0.5% 123 SDS. Cell lysates were then incubated at 56°C for 3 h in the presence of 100 µg/mL 124 of proteinase K. DNA was purified by successive phenol/chloroform extractions and 125 the resultant aqueous phase was mixed with 3M sodium acetate (pH 5.2) and absolute 126 ethanol. The mixture was incubated at -20°C overnight and the ethanol-precipitated 127 DNA was washed with 70% ethanol. Purified DNA was resuspended in 10 mM 128 Tris-HCl, pH 7.5, 1 mM EDTA and treated with 50 µg/mL DNase-free RNase A for 129 1 h. Samples were resolved on a 1% agarose gel and stained with 0.5  $\mu$ g/mL ethidium 130 bromide before DNA was visualized with ultraviolet light (21).

132	DAPI (40, 6-diamidino-2-phenylindole dihydrochloride) Staining. Cells were
133	seeded onto a 12-well plate at a density of 5 x $10^4$ cells/well before treating with drugs.
134	Hep3B cells were cultured with vehicle alone or 45 $\mu$ M hispolon in DMEM medium
135	for 24, 48, and 72 h. After the treatment, cells were fixed with 3.7% formaldehyde for
136	15 min, permeabilized with 0.1% Triton X-100 and stained with 1 $\mu g/mL$ DAPI for 5
137	min at 37 °C. The cells were then washed with PBS and examined by fluorescence
138	microscopy (Nikon, Tokyo, Japan).
139	
140	Flow Cytometric Analysis for Cell Cycle Distribution. Human hepatocellular
141	carcinoma Hep3B cells (1 x $10^6$ cells) were suspended in a hypotonic solution (0.1%
142	Triton X-100, 1 mM Tris-HCl (pH 8.0), 3.4 mM sodium citrate, and 0.1 mM EDTA)
143	and stained with 50 $\mu\text{g}/\text{mL}$ of propidium iodide (PI). DNA content was analyzed with
144	a FACScan (Becton Dickinson, San Jose, CA). The population of cells in each phase
145	of cell cycle was determined using CellQuest PRO software (Becton Dickinson, San

146 Jose, CA).

147

148 Assay of Cell Apoptosis. Quantitative assessment of apoptosis was analyzed by an 149 Annexin V-FITC assay kit (BD Biosciences, San Jose, CA). Briefly, cells grown in 10

150	cm Petri dishes were harvested with trypsin and washed in PBS. Cells were then
151	resuspended in a binding buffer (10 mM HEPES/NaOH (pH 7.4), 140 mM NaCl, 2.5
152	mM CaCl <sub>2</sub> ) and stained with Annexin V-FITC and PI at room temperature for 15 min
153	in the dark. Cells were analyzed in an EPICS flow cytometer (Coulter Electronics)
154	within 1 h after staining. Data from 10,000 cells were detected for each data file.
155	Early apoptotic cells were defined as Annexin V-FITC-positive and PI-negative cells
156	(Annexin V+/PI- fraction) and late apoptosis or necrotic cells were defined as annexin
157	V+/PI+ cells.

158

**Preparation of Whole-Cell Lysates.** Hep3B cells  $(1 \times 10^5 \text{ cells})$  were plated in a 159 100-mm Petri dish and were treated with various concentrations of hispolon. Hep3B 160 161 cells were washed twice with PBS and were scraped into a microcentrifuge tube. The 162 cells were centrifuged at 1,250g for 5 min, and the pellet was lysed with iced-cold RIPA (Radio-Immunoprecipitation Assay) buffer (1% NP-40, 50 mM Tris-base, 0.1% 163 SDS, 0.5% deoxycholic acid, 150 mM NaCl, pH 7.5), to which was added freshly 164 prepared phenylmethylsulfonyl fluoride (10 mg/mL), leupeptin (17 mg/mL), and 165 166 sodium orthovanadate (10 mg/mL). After incubation for 5 min on ice, the samples were centrifuged at 10,000g for 10 min, and then the supernatants were collected as 167 whole-cell lysates. The lysates were denatured and subjected to SDS-PAGE and 168

169 Western blotting. The protein content was determined with Bio-Rad protein assay170 reagent using BSA as a standard.

171

172 Western Blotting Analysis. Whole-cell lysates proteins (30-50 µg of partially 173 purified protein) were mixed with an equal volume of electrophoresis sample buffer, 174 and the mixture was then boiled for 10 min. Then, an equal protein content of total cell lysate from control, 0.2% DMSO, and hispolon-treated sample were resolved on 175 10-12% SDS-PAGE gels. Proteins were then transferred onto nitrocellulose 176 177 membranes (Millipore, Bedford, MA) by electroblotting using an electroblotting apparatus (Bio-Rad). Nonspecific binding of the membranes was blocked with 178 179 Tris-buffered saline (TBS) containing 1% (w/v) nonfat dry milk and 0.1% (v/v) 180 Tween-20 (TBST) for more than 2 h. Membranes were washed with TBST three 181 times each for 10 min and then incubated with an appropriate dilution of specific 182 primary antibodies in TBST overnight at 4 °C. The membranes were washed with 183 TBST and then incubated with an appropriate secondary antibody (horseradish peroxidase-conjugated, goat antimouse, or antirabbit IgG) for 1 h. After washing the 184 185 membrane three times for 10 min in TBST, the bands were visualized using ECL reagents (Millipore, Billerica, MA). Band intensity on scanned films was quantified 186

using Kodak Molecular imaging (MI) software and expressed as relative intensitycompared with control.

189

190Statistical Analysis. Values are expressed as means  $\pm$  SD and analyzed using191one-way ANOVA followed by LSD Test for comparisons of group means. All192statistical analyses were performed using SPSS for Windows, version 10 (SPSS, Inc.);193a P value <0.05 is considered statistically significant.</td>

194

## 195 **RESULTS**

**Isolation of hispolon from PL and its Structural characterization.** PL was isolated via extensive chromatographic purification of the ethyl acetate-soluble fraction of the dried fruiting body. The chemical structure of the purified yellow powder was elucidated by NMR spectroscopy and mass spectrometry studies and was identified as hispolon.

201

Inhibitory Effects of Hispolon on Tumor Cell Growth. To examine whether
hispolon would alter malignant proliferation, inhibitory effects on the growth of J5,
HepG2, and Hep3B tumor cells were determined by a MTT colorimetric assay. As

205	shown in Fig. 1, hispolon inhibited cellular growth of J5, HepG2, and Hep3B cells in
206	a time-dependent and dose-dependent manner, and treatment for 24, 48 and 72 h
207	induced marked inhibition of cellular growth. The $IC_{50}$ values (50% cell growth
208	inhibitory concentration) at 72 h for human hepatoma cancer cells J5, HepG2, and
209	Hep3B cells were 54.53 $\pm$ 0.63, 87.59 $\pm$ 1.42, and 35.90 $\pm$ 1.10 $\mu M,$ respectively
210	(Table 1). As compared to J5 and HepG2 cells, hispolon seemed to have a stronger
211	death effect toward Hep3B liver cancer cells. The results indicate that hispolon was
212	more cytotoxic to Hep3B cells.
213	
214	Effects of Hispolon on Nuclear DNA Fragmentation of Hep3B Cells. We assessed
215	the effect of hispolon on the induction of apoptosis in Hep3B cells by DNA
215 216	the effect of hispolon on the induction of apoptosis in Hep3B cells by DNA fragmentation assay. Hep3B cells treated with 22.5, 45, and 66.5 $\mu$ M hispolon for 48
216	fragmentation assay. Hep3B cells treated with 22.5, 45, and 66.5 $\mu$ M hispolon for 48
216 217	fragmentation assay. Hep3B cells treated with 22.5, 45, and 66.5 $\mu$ M hispolon for 48 h, or treated with 45 $\mu$ M for 24, 48 and 72 h showed that hispolon treatment resulted
<ul><li>216</li><li>217</li><li>218</li></ul>	fragmentation assay. Hep3B cells treated with 22.5, 45, and 66.5 $\mu$ M hispolon for 48 h, or treated with 45 $\mu$ M for 24, 48 and 72 h showed that hispolon treatment resulted in the formation of DNA fragments. Nucleosomal DNA fragmentation was observed
<ul><li>216</li><li>217</li><li>218</li><li>219</li></ul>	fragmentation assay. Hep3B cells treated with 22.5, 45, and 66.5 $\mu$ M hispolon for 48 h, or treated with 45 $\mu$ M for 24, 48 and 72 h showed that hispolon treatment resulted in the formation of DNA fragments. Nucleosomal DNA fragmentation was observed in cells treated with 45 $\mu$ M of hispolon for 0, 24, 48, and 72 h or treated with 22.5, 45,
<ul> <li>216</li> <li>217</li> <li>218</li> <li>219</li> <li>220</li> </ul>	fragmentation assay. Hep3B cells treated with 22.5, 45, and 66.5 $\mu$ M hispolon for 48 h, or treated with 45 $\mu$ M for 24, 48 and 72 h showed that hispolon treatment resulted in the formation of DNA fragments. Nucleosomal DNA fragmentation was observed in cells treated with 45 $\mu$ M of hispolon for 0, 24, 48, and 72 h or treated with 22.5, 45, and 66.5 $\mu$ M hispolon for 48 h (Fig. 2A). The profile for hispolon-induced apoptosis

224 Effects of Hispolon on Phenotypic Changes in Cell Nucleus. This study further 225 elucidated whether hispolon also induces DNA fragmentation and chromatin 226 condensation in Hep3B cells. Treatment with hispolon resulted in changes in nuclear morphology, as demonstrated by DAPI staining. Condensation and fragmentation 227 were seen in cells 24, 48, and 72 h after 45 µM of hispolon treatment (Fig. 2B). The 228 229 phenotypic characteristic of hispolon-treated Hep3B cells was also evaluated by 230 microscopic inspection of overall morphology. Apoptotic bodies were observed after 231 Hep3B cells were treated with hispolon for 24 h. Based on the above data, DNA 232 condensation and formation of apoptotic bodies indicated that hispolon-induced 233 Hep3B cell death was a typical apoptotic cell death.

234

235 Effects of Hispolon on Cell Cycle Distribution. Induction of apoptosis has been 236 reported to be a potentially promising approach for cancer therapy. Exhibition of the 237 biological phenomena (cell cycle redistribution, DNA fragmentation, and chromatin 238 condensation) represents the proceeding of apoptosis (22). The apoptotic effect of hispolon was confirmed by flow cytometric analysis. As shown in Fig. 3A, 239 240 concomitant with the growth inhibitory effect, hispolon treatment induced a strong 241 S-phase arrest in a time-dependent manner. When Hep3B cells were incubated with 242 45 µM of hispolon for 0, 6, 12, and 24 h, the relative percentage of cells staying at the S phase were 17.31%, 43.95%, 70.98% and 70.89%, respectively (Fig. 3B). This increase in the S-phase cell population was accompanied by a concomitant decrease in the G0/G1 and G2/M phase cell populations. Meanwhile, the sub-G1 population was slightly increased in cells exposed to 45  $\mu$ M hispolon. These results indicated that hispolon caused cell cycle arrest at the S phase, followed by apoptosis.

248

249 Effects of Hispolon on Cell Apoptosis. To further confirm and quantify the 250 apoptosis of Hep3B cells triggered by hispolon, cells were stained with both Annexin 251 V-FITC and PI, and subsequently analyzed by flow cytometry (5). Fig. 4 shows the 252 annexin V-FITC/PI analysis of Hep3B cells cultured with 45 µM of hispolon for 0, 6, 253 12 and 24 h. Annexin V positive cells were considered as the relative amount of 254 apoptoic cells. Early apoptotic cells appeared in the annexin V+/PI- fraction, whereas 255 cells damaged by scraping appeared in the annexin V-/PI+ fraction, and late 256 apoptosis or necrotic cells were evident in the annexin V+/PI+ fraction. After treatment with 45 µM of hispolon for 0, 6, 12, and 24 h, the corresponding quantities 257 of necrosis and apoptosis were 1.2%, 5.4%, 14.4%, and 19.6%, respectively (Annexin 258 259 V+/PI+ fraction).

260

261 Hispolon Induces Apoptosis via Intrinsically- and Extrinsically-Mediated

Pathways. The effects of hispolon on the protein expression of Fas, FasL, pro-caspase-8, and Bid in Hep3B cells are shown in Fig. 5A and 5B. Treatment of Hep3B cells with hispolon (45  $\mu$ M) for 0, 3, 6, 12, and 24 h resulted in significant increases in the levels of Fas and FasL expression. Treatment with 45  $\mu$ M hispolon for 24 h significantly decreased the expression levels of pro-caspase-8 and Bid by 48% and 56%, respectively, as compared to those of the control.

268 The effects of hispolon on the protein expression of the Bcl-2 family and cytosolic cytochrome c in Hep3B cells are shown in Fig. 6A and 6B. After treatment with 45 269 270 µM hispolon for 24 h, the level of pro-apoptotic protein expression of Bax was 271 increased by 187.7%, in comparison to the control. Hispolon treatment at 45 µM for 272 24 h significantly decreased the level of Bcl-2 (antiapoptotic protein) expression by 273 38% in comparison with the control. Cytochrome c release in the cytosolic fraction 274 following hispolon treatment was then investigated. Treatment with hispolon (45 µM, 275 24 h) resulted in a significant increase in the level of cytosolic cytochrome c276 expression by 177%, as comparison to the control. A significant time-dependent shift 277 in the ratio of Bax to Bcl-2 was observed after hispolon treatment at 45 µM for 0-24 h 278 (Fig. 6B).

The effects of hispolon on the protein expression of pro-caspase-3, caspase-9,
and poly (ADP-ribose) polymerase (PARP) in Hep3B cells are shown in Fig.7A and

281	7B. The results show that exposure of Hep3B cells to hispolon (45 $\mu M,$ 24 h) caused
282	the degradation of pro-caspase-3 and caspase-9, which generated a fragment of
283	caspase-9 and caspase-3. Hispolon treatment at 45 $\mu$ M for 24 h significantly increased
284	the level of expression of cleaved PARP by 138%, as comparison to the control. The
285	results indicate that hispolon treatment causes a significant increase in the activity of
286	caspase-9 and caspase-3 and hispolon may have acted through initiator caspase-8 and
287	then executioner caspase-3 to increase the cleavage form of PARP.
288	
289	Effects of Hispolon on the Expression of Cell Cycle Regulators Involved in
290	<b>S-Phase Arrest.</b> As shown by immunoblot analysis in Fig. 8A, hispolon (45 µM, 24 h)
290	<b>5-1 hase Arrest.</b> As shown by minunoolot analysis in Fig. 6A, inspoton (+5 $\mu$ Wi, 24 ii)
290	treatment caused a time-dependent decrease in the expression levels of cell cycle
291	treatment caused a time-dependent decrease in the expression levels of cell cycle
291 292	treatment caused a time-dependent decrease in the expression levels of cell cycle regulators including cyclin A, cyclin E and cyclin-dependent kinases CDK 2, which
291 292 293	treatment caused a time-dependent decrease in the expression levels of cell cycle regulators including cyclin A, cyclin E and cyclin-dependent kinases CDK 2, which may contribute to the cell cycle progression from G0/G1 to S-phase. Hispolon
291 292 293 294	treatment caused a time-dependent decrease in the expression levels of cell cycle regulators including cyclin A, cyclin E and cyclin-dependent kinases CDK 2, which may contribute to the cell cycle progression from G0/G1 to S-phase. Hispolon treatment at 45 $\mu$ M for 24 h significantly decreased the level of expression of cyclin A,
291 292 293 294 295	treatment caused a time-dependent decrease in the expression levels of cell cycle regulators including cyclin A, cyclin E and cyclin-dependent kinases CDK 2, which may contribute to the cell cycle progression from G0/G1 to S-phase. Hispolon treatment at 45 $\mu$ M for 24 h significantly decreased the level of expression of cyclin A, cyclin E, and CDK 2 by 48.3%, 61.2% and 42.2%, respectively, in comparison with
<ul> <li>291</li> <li>292</li> <li>293</li> <li>294</li> <li>295</li> <li>296</li> </ul>	treatment caused a time-dependent decrease in the expression levels of cell cycle regulators including cyclin A, cyclin E and cyclin-dependent kinases CDK 2, which may contribute to the cell cycle progression from G0/G1 to S-phase. Hispolon treatment at 45 $\mu$ M for 24 h significantly decreased the level of expression of cyclin A, cyclin E, and CDK 2 by 48.3%, 61.2% and 42.2%, respectively, in comparison with the control. Binding of cyclins to CDKs would form active kinase complexes, which

300 time-dependent manner by hispolon treatment. Hispolon treatment at 45  $\mu$ M for 24 h 301 significantly increased the level of expression of p21waf1/Cip1 and p27Kip1 by 156% 302 and 144% in comparison with the control.

303

304 Effects of Hispolon on MAPK Signaling Pathway. Studies have shown that the 305 MAPK signaling pathway plays an important role in the action of chemotherapeutic 306 drugs (23). Therefore, we determined whether the MAPKs were activated in 307 hispolon-treated Hep3B cells by Western blot analysis using specific antibodies against the phosphorylated (activated) forms of the kinases. It was found that hispolon 308 309 treatment induced differential phosphorylation of JNK, ERK, and p38 MAPK in cells 310 exposed to 45 µM hispolon (Fig. 9A and 9B). Phosphorylation of ERK was detected 311 as a sustained activation from 0 to 24 h, which decreased thereafter and reached the 312 control level at 24 h. Activation of p38 by hispolon was also observed as early as 3 h 313 after hispolon treatment, which peaked at approximately 24 h. A time course study 314 showed that JNK activation displayed a rapid onset after 3h of treatment, followed by 315 a progressive decline, returning to the basal level after 24 h. 316 To study the role of MAPK activation in hispolon-induced growth inhibition, we

examined the effects of specific MAPK inhibitors on overall cell death. The results ofthe MTT assay showed that pretreatment with SP600125 (a JNK inhibitor) or

319 SB203580 (a p38 inhibitor) had no effect on hispolon-induced cell death (Fig. 9C),

320 although these inhibitors reduced the phosphorylation of their target kinases.

321 The results suggested that JNK and p38 did not play important roles in regulating cell death in Hep3B cells induced by hispolon. However, pretreatment with PD98059 322 323 (an ERK inhibitor) significantly decreased the extent of cell death induced by 324 hispolon (Fig. 9C). Only the ERK inhibitor PD98059 significantly blocked 325 hispolon-mediated cell death. These contradictory results imply that the drug actions 326 of hispolon indeed result from the complex interaction of many compounds and many 327 targeted molecules. These results suggested that activation of the ERK pathway was 328 involved in the apoptotic cell death of Hep3B cells induced by hispolon.

329

330

# 331 Discussion

In the present study, we investigated the apoptosis of human hepatocellular carcinoma cells induced by hispolon. Our data revealed that hispolon, a phenol compound, acts directly on human hepatocellular carcinoma cancer cells to induce cytotoxicity in a manner that causes apoptosis (Table 1). In breast and bladder cancer cells, Lu et al. have reported that hispolon treatment for 72 h inhibits the cell viability at IC<sub>50</sub> values ranging from 20  $\mu$ M-40  $\mu$ M (24) as well as inhibits the growth of human gastric cancer cells cells in a dose- and time-dependent manner, with an  $IC_{50}$ of 30  $\mu$ M at 72 h of incubation (25).

340	A flow cytometic analysis of PI -labeled cells shows that treating Hep3B cells
341	with hispolon (45 $\mu$ M) induced significant accumulation of cells in the S phase (Fig.
342	3A). The ratio of $G_0/G_1$ to S to $G_2/M$ phase in Hep3B cells at 0, 6, 12, and 24 h varied
343	significantly in the presence of 45 $\mu M$ (Fig. 3B). The $G_0/G_1$ cell population increased
344	to 70.89% in Hep3B cells treated with 45 $\mu M$ of hispolon for 24 h. Moreover, a
345	characteristic hypodiploid DNA content peak (sub-G1) was easily detected after
346	treatment with hispolon 45 $\mu$ M for 0, 6, 12, and 24 h. A significant increase in sub-G <sub>1</sub>
347	phase is indicative of induction of apoptosis. Uncontrolled cell proliferation is the
348	hallmark of cancer, and tumor cells have typically acquired mutations in genes that
349	directly regulate their cell cycle (26-27).
350	Inhibition of deregulated cell cycle progression in cancer cells is an effective

Inhibition of deregulated cell cycle progression in cancer cells is an effective strategy to halt tumor growth (28). Cyclins, CDKs, and CDKIs play essential roles in the regulation of cell cycle progression. CDKIs, such as p21waf1/Cip1 and p27Kip1, are tumor suppressor proteins that downregulate the cell cycle progression by binding with active cyclin-CDK complexes and thereby inhibiting their activities (29). Chemopreventive agents usually cause apoptosis or cell cycle arrest at the G0/G1 or G2/M phases. Relatively little is known about mechanisms that control progress

357	within the S-phase. It has been reported that hispolon elicits cell-cycle arrest at G2-M
358	phases in human breast and bladder cancer cells through the induction of CDKIs and
359	the inhibition of cyclins and CDKs (24). Although these results offer much insight for
360	the cell cycle arrest action of hispolon, the detailed molecular mechanisms remain to
361	be clarified. It has been reported that S-phase cell cycle arrest occurs with the loss of
362	Cdk2 activity due to reduced formation of active complex cyclin E/Cdk2 kinase (30).
363	We demonstrate here that hispolon-induced cell-cycle arrest was accompanied by
364	down-regulating the protein levels of cyclin A, cyclin E, and CDK2 and up-regulation
365	of p21 and p27 in Hep3B cells. It has been reported that S phase cell-cycle arrest
366	occurs with the loss of Cdk2 activity due to up-regulation of p21 and reduced
367	formation of active complex cyclin E/Cdk2 kinase (23). Our findings that hispolon
368	down-regulated cyclin A, cyclin E and CDK2 but up-regulated p21 and p27 suggest
369	that S-phase arrest is responsible for the cell-cycle-arresting effect of hispolon in
370	Hep3B cells.

Hispolon-induced apoptosis in Hep3B cells was also indicated by DNA laddering (Fig. 2A) and DAPI positive staining (Fig. 2B). The induction of apoptosis stimulates endonucleases, which catalyze the breakage of double-stranded DNA to form fragments with oligonucleosome-length, resulting in a typical DNA electrophoresis ladder that signifies apoptotic cell death (*26*). The apoptosis-inducing effect of

376	hispolon on Hep3B cells appeared to be directly proportional to its concentration. In
377	addition, the apoptosis-inducing efficacy of hispolon was found to be similar to its
378	anti-porliferative activity toward Hep3B cells. Furthermore, using annexin V-FITC to
379	identify apoptotic cells by binding to phosphatidyl serine and a red-fluorescent PI to
380	bind to nucleic acids of necrotic cells, the present study further demonstrated that
381	hispolon induced a significant and dose-dependent increase of annexin $V^{\!+}\!/PI^{\!+}$
382	apoptotic cells (Fig. 4).

383 Caspases are believed to play crucial roles in mediating various apoptotic 384 responses. A model involving two different caspases (caspase-8 and -9) in the 385 mediation of distinct types of apoptotic stimuli has been proposed (31). The cascade 386 led by caspase-8 is involved in death receptor-mediated apoptosis such as the one 387 triggered by Fas. Ligation of Fas by Fas ligand results in sequential recruitment of 388 FADD (Fas-associated death domain) and procaspase-8 to the death domain of Fas to 389 form the death-inducing signaling complex, leading to cleavage of procaspase-8, with 390 the consequent generation of active caspase-8. Active caspase-8 in turn activates 391 downstream effecter caspases through the cleavage of Bid, committing the cell to 392 apoptosis (27). The present results suggest that hispolon may act through the initiator 393 caspase-8 and then the executioner caspase-3 to increase the cleavage form of PARP 394 for DNA fragmentation (Fig. 5A and 7A).

395	Many reports have pointed out that the ability of anticancer agents in inducing
396	apoptosis of tumor cells (such as Taxol) correlates with the ability of decreasing the
397	expression of Bcl-2 (32). In the present study, we showed that the expression of Bcl-2
398	decreased as the concentration of hispolon and the percentage of apoptotic Hep3B
399	cells increased. This inverse proportional relationship suggested that Bcl-2 may play a
400	preventive role in hispolon-mediated apoptosis of Hep3B cells.
401	Mitochondrial-dependent apoptosis is often through the activation of a pro-apoptotic
402	factor in the Bcl-2 family. Thus, one possible role of Bcl-2 in the prevention of
403	apoptosis is to block the release of cytochrome $c$ from mitochondria (Fig. 6A). On the
404	contrary, increases in the expression of Bax and cytochrome $c$ release were observed
405	during hispolon treatment in the present study. Bax is a pro-apoptotic protein that has
406	also been shown to induce cytochrome $c$ release and caspase activation recently (33).
407	The above findings suggest that hispolon induces apoptosis in Hep3B cells through a
408	mitochondria-mediated pathway.
409	Several protein kinase pathways have been known to regulate cell proliferation

and survival. MAPKs, a family of serine-threonine protein kinases, have been
implicated in apoptosis and cell cycle regulation signaling in diverse cell models (*23*).
In general, JNK and p38 are activated by diverse stimuli such as oxidative stress, UV
irradiation, and osmotic shock and required for the induction of apoptosis. ERK plays

414 vital roles in cell growth and division and is generally considered to be a survival 415 mediator (34). In human HCC cell lines, multiple anticancer effects such as inhibition 416 of cellular proliferation as well as induction of cell cycle arrest and apoptosis have 417 been achieved by blocking ERK signaling (35). ERK inactivation observed in this 418 study may contribute to the S phase cell cycle arresting and apoptotic activities of hispolon, which need to be investigated further. In addition, different MAPK 419 420 signaling pathways can be coordinately manipulated to enhance the efficacy of 421 anticancer drug. Cotreatment of anticancer drugs with ERK inhibitors has been found 422 to enhance anticancer effects. In our experiments, as shown in Fig. 9A, hispolon markedly elevated the phosphorylated forms of JNK and p38 and reduced the 423 424 phosphorylated form of ERK1/2 in a dose dependent manner. Therefore, 425 hispolon-induced apoptosis in Hep3B involves mitochondria caspase pathways, 426 activation of JNK and P38 and inhibition of the ERK MAPK signaling. The use of 427 specific inhibitors revealed that JNK and p38 did not play important roles in regulating cell death induced by hispolon in Hep3B cells. In this study, the MTT 428 method was used to examine the effects of specific MAPK inhibitors, as the same 429 430 method has often been used to examine the effects of specific MAPK inhibitors (23, 431 36, 37). In our previous reports, we also used the same approach to show that hispolon 432 modulates ERK phosphorylation (20, 23).

433	Our observations that hispolon induced S-phase arrest and p21 overexpression
434	are in agreement with those of a previous report which shows that the transduction of
435	the p21 gene results in S-phase arrest (40). P21, an inhibitor of CDKs, directly inhibits
436	CDK2, CDK3, CDK4, and CDK6 activity. Overexpression of p21 usually leads to $G_1$
437	or G <sub>2</sub> arrest by inhibiting CDK activity. P21 can also directly inhibit DNA synthesis
438	by binding to proliferating cell nuclear antigen (PCNA) (41). The expression of p21
439	can be regulated at the transcriptional, post-transcriptional, or post-translational levels
440	by p53-dependent and -independent mechanisms (5). Indeed, we found that
441	suppression of ERK activation attenuated hispolon-mediated induction of p21
442	expression and S-phase arrest. Although ERK and p21 are likely to play a role in
443	hispolon-mediated S-phase arrest, it is possible that some other molecules that were
444	not examined here may also be involved in hispolon-mediated S-phase arrest.
445	In conclusion, this study has provided mechanistic insights into how hispolon
446	regulates the components of cell cycle progression and apoptotic machinery to delay S
447	to G2/M transition and induces apoptosis in Hep3B cells. Our data imply the potential
448	of hispolon as a chemotherapeutic agent because many antbicancer drugs are known
449	to achieve their anticancer function by inducing apoptosis and/or cell cycle arrest in
450	susceptible cells.

#### 452 ABBREVIATIONS USED

FBS, fetal bovine serum; MTT, 3-(4,5-dimethylthiazol-2-yl)-2,5-diphenyltetrazolium
bromide; PARP, poly(ADP-ribose) polymerase; MAPK, mitogen-activated protein
kinase; ERK, extracellular signaling-regulating kinase; JNK/SAPK, c-Jun N-terminal
kinase/ stress-activated protein kinase;

457

### 458 ACKNOWLEDGEMENTS

459 The authors want to thank the financial supports from the National Science Council

460 (NSC 97-2313-B-039 -001 -MY3), China Medical University (CMU) (CMU97-232

- 461 and CMU99-S-29) and and Taiwan Department of Health Clinical Trial and Research
- 462 Center of Excellence (DOH100-TD-B-111-004) and the Cancer Research Center of
- 463 Excellence (DOH100-TD-C-111-005).
- 464

#### 465 LITERATURE CITED

- 466 (1) Anthony, P. P. Hepatocellular carcinoma: an overview. *Histopathology* 2001, 39,
  467 109–118.
- 468 (2) Hengartner, M. O. The biochemistry of apoptosis. *Nature* **2000**, *407*, 770-776.
- 469 (3) Earnshaw, W. C.; Martins, L. M.; Kaufmann, S. H. Mammalian caspases:

- 470 structure, activation, substrates, and functions during apoptosis. *Annu. Rev.*471 *Biochem.* 1999, 68, 383-424.
- 472 (4) Suda, T.; Takahashi, T.; Golstein, P.; Nagata, S. Molecular cloning and expression
  473 of the Fas ligand, a novel member of the TNF family. *Cell* **1993**, *75*, 1169-1178.
- 474 (5) Pan, M. H; Chang, Y. H.; Badmaev, V.; Nagabhushanam, K.; Ho, C. T.
  475 Pterostilbene induces apoptosis and cell cycle arrest in human gastric carcinoma
  476 cell. *J. Agric. Food Chem.* 2007, *55*, 7777-7785.
- 477 (6) Nicholson, D. W.; Thornberry, N. A. Caspases: killer proteases. *Trends Biochem*.
- 478 *Sci.* **1997**, *22*, 299-306.
- (7) Shimizu, S.; Narita, M.; Tsujimoto, Y. Bcl-2 family proteins regulate the release of
  apoptogenic cytochrome *c* by the mitochondrial channel VDAC. *Nature* 1999, *399*,
  481 483-487.
- (8) Katdare, M.; Jinno, H.; Osborne, M. P.; Telang, N. T. Negative growth regulation
  of oncogene-transformed human breast epithelial cells by phytochemicals: Role of
  apoptosis. *Ann. NY Acad. Sci.*1999, 889, 247-252.
- 485 (9) Park, H. G.; Shim, Y. Y.; Choi, S. O.; Park, W. M. New method development for
- 486 nanoparticle extraction of water-soluble beta-(1-->3)-D-glucan from edible
- 487 mushrooms, Sparassis crispa and Phellinus linteus. J. Agric. Food Chem. 2009,
- 488 57, 2147-2154.
- 489 (10) Guo, J.; Zhu, T.; Collins, L.; Xiao, Z. X.; Kim, S. H.; Chen, C.Y. Modulation of
- 490 lung cancer growth arrest and apoptosis by *Phellinus Linteus*. *Mol. Carcinogen*.
- **2007**, *46*, 144–154.
- 492 (11) Lee, H. J.; Lim, E. S.; Ahn, K. S.; Shim, B. S.; Kim, H. M.; Gong, S. J.; Kim, D.

- 493 K.; Kim, S. H. Cambodian *Phellinus linteus* inhibits experimental metastasis of
- 494 melanoma cells in mice via regulation of urokinase type plasminogen activator.
- 495 *Biol. Pharmaceut. Bull.* **2005**, *28*, 27–31.
- 496 (12) Sliva, D.; Jedinak, A.; Kawasaki, J.; Harvey, K.; Slivova, V. Phellinus linteus
- 497 suppresses growth, angiogenesis and invasive behaviour of breast cancer cells
- through the inhibition of AKT signaling. *Br. J. Cancer* 2008, 98, 1348–1356.
- 499 (13) Ali, N. A.; Ludtke, J.; Pilgrim, H.; Lindequist, U. Inhibition of
- 500 chemiluminescence response of human mononuclear cells and suppression of
- 501 mitogen-induced proliferation of spleen lymphocytes of mice by hispolon and
- 502 hispidin. *Pharmazie* **1996**, *51*, 667–670.
- 503 (14) Venkateswarlu, S.; Ramachandra, M. S.; Sethuramu, K.; Subbaraju, G. V.
- 504 Synthesis and antioxidant activity of hispolon, a yellow pigment from *Inonotus*
- 505 *hispidius. Indian J. Chem. B Org.* **2002,** *41*, 875-877.
- 506 (15) Hung, W. C.; Chang, H. C. Indole-3-carbinol inhibits Sp1-induced matrix
  507 metalloproteinase-2 expression to attenuate migration and invasion of breast
  508 cancer cells. *J. Agric. Food Chem.* 2009, *57*, 76–82.
- 509 (16) Lin, K. H.; Lin, Y. W.; Lee, H. F.; Liu, W. L.; Chen, S. T.; Cheng, S. Y.
- 510 Increased invasive activity of human hepatocellular carcinoma cells is associated
- 511 with an overexpression of thyroid hormone  $\beta$ 1 nuclear receptor and low

expression of the anti-metastatic nm23 gene. Cancer Lett. 1995, 98, 89–95.

513	(17) Cheng, S.; Alfonso-Jaume, M. A.; Mertens, P. R.; Lovett, D. H. Tumour
514	metastasis suppressor, nm23-beta, inhibits gelatinase A transcription by
515	interference with transactivator Y-box protein-1 (YB-1). Biochem. J. 2002, 366,
516	807-816.
517	(18) Ohba, K.; Miyata, Y.; Koga, S.; Kanda, S.; Kanetake, H. Expression of nm23-H1
518	gene product in sarcomatous cancer cells of renal cell carcinoma: correlation with
519	tumor stage and expression of matrix metalloproteinase-2, matrix
520	metalloproteinase-9, sialyl Lewis X, and c-erbB-2. Urology 2005, 65, 1029-1034.

- (19) Murakami, M.; Meneses, P. I.; Lan, K.; Robertson, E. S. The suppressor of
  metastasis Nm23-H1 interacts with the Cdc42 Rho family member and the
  pleckstrin homology domain of oncoprotein Dbl-1 to suppress cell migration. *Cancer Biol. Ther.* 2008, 7, 677-688.
- 525 (20) Huang, G. J.; Yang, C. M.; Chang, Y. S.; Amagaya, S.; Wang, H. C.; Hou, W. C.;
- 526 Huang, S. S.; Hu, M. L. Hispolon suppresses SK-Hep1 human hepatoma cell
- 527 metastasis by inhibiting matrix metalloproteinase-2/9 and urokinase-plasminogen
- 528 activator through the PI3K/Akt and ERK signaling pathways. J. Agric. Food
- 529 *Chem.* **2010**, *58*, 9468-9475.
- (21) Huang, G. J.; Sheu, M. J.; Chen, H. J.; Chang, Y. S.; Lin, Y. H. Growth Inhibition
  and Induction of Apoptosis in NB4 Promyelocytic Leukemia Cells by Trypsin
  Inhibitor from Sweet Potato Storage Roots. J. Agric. Food Chem. 2007, 55,
  2548-2553.

534	(22) Pan, M. H.; Lin, C. C.; Lin, J. K.; Chen, W. J. Tea Polyphenol
535	(–)-epigallocatechin 3-gallate suppresses heregulin- $\beta$ 1-induced fatty acid synthase
536	expression in human breast cancer cells by inhibiting phosphatidylinositol
537	3-Kinase/Akt and mitogen-activated protein kinase cascade signaling. J. Agric.
538	Food Chem. 2007, 55, 5030–5037.

- 539 (23) Chen, T.; Wong, Y. S. Selenocystine Induces S-Phase Arrest and Apoptosis in
- 540 Human Breast Adenocarcinoma MCF-7 Cells by Modulating ERK and Akt
- 541 Phosphorylation. J. Agric. Food Chem. 2008, 56, 10574–10581.
- 542 (24) Lu, T. L.; Huang, G. J.; Lu, T. J.; Wu, J. B.; Wu, C. H.; Yang, T. C.; Iizuka, A.;
  543 Chen, Y. F. Hispolon from *Phellinus linteus* has antiproliferative effects via
  544 MDM2-recruited ERK1/2 activity in Breast and Bladder Cancer Cells. *Food*545 *Chem. Toxicol.*2009, 47, 2013-2021.
- 546 (25) Chen, W.; Zhao, Z.; Li, L.; Wu, B.; Chen, S. F.; Zhou, H.; Wang, Y.; Li, Y. Q.
- 547 Hispolon induces apoptosis in human gastric cancer cells through a
- 548 ROS-mediated mitochondrial pathway. *Free Radic. Biol. Med.* **2008**, *45*, 60-72.
- 549 (26) Chen, W. J.; Lin, J. K. Mechanisms of cancer chemoprevention by hop bitter
- acids (beer aroma) through induction of apoptosis mediated by Fas and caspase
  cascades. *J. Agric. Food Chem.* 2004, *52*, 55-64.
- 552 (27) Song, T. Y.; Hsu, S. L.; Yeh, C.T.; Yen, G. C. Mycelia from *Antrodia camphorata*553 in submerged culture induce apoptosis of human hepatoma HepG2 cells possibly
  554 through regulation of Fas pathway. *J. Agric. Food Chem.* 2005, *53*, 5559-5564.

- 555 (28) Yeh, T. C.; Chiang, P. C.; Li, T. K.; Hsu, J.L.; Lin, C. J.; Wang, S. W.; Peng, C. Y.;
- Guh, J. H. Genistein induces apoptosis in human hepatocellular carcinomas via
  interaction of endoplasmic reticulum stress and mitochondrial insult. *Biochem. Pharmacol.* 2007, *15*, 782-792.
- (29) Hsu, Y. L.; Uen, Y. H.; Chen, Y.; Liang, H. L.; Kuo, P. L. Tricetin, a Dietary
  Flavonoid, Inhibits Proliferation of Human Breast Adenocarcinoma MCF-7 Cells
  by Blocking Cell Cycle Progression and Inducing Apoptosis. *J. Agric. Food Chem.* 2009, *57*, 8688–8695.
- 563 (30) Chen, X.; Lv, P.; Liu, J.; Xu, K. Apoptosis of human hepatocellular
- 564 carcinoma cell (HepG2) induced by cardiotoxin III through S-phase arrest. *Exp*.
- 565 *Toxicol. Pathol.* **2009**, *61*, 307-315.
- 566 (31) Yeh, C. T.; Yen, G. C. Induction of apoptosis by the anthocyanidins through
- 567 regulation of Bcl-2 gene and activation of c-Jun N-terminal kinase cascade in
- 568 hepatoma cells. J. Agric. Food Chem. 2005, 53, 5559-5564.
- (32) Vermes, I.; Haanen, C.; Steffens-Nakken, H.; Reutlingsperger, CPM. A novel
  assay for aptosis flow cytometric detection of phosphatidyl serine expression on
  early apoptotic cells using labelled annexin V. *J. Immunol. Methods* 1995, *184*,
  39–51.
- (33) Hsu, C. L.; Lo, W. H.; Yen, G. C. Gallic acid induces apoptosis in 3T3-L1
  pre-adipocytes via a Fas- and mitochondrial-mediated pathway. *J. Agric. Food Chem.* 2007, 55, 7359-7365.
- 576 (34) Wang, S. Y.; Feng, R.; Bowman, L.; Penhallegon, R.; Ding, M.; Lu, Y.
- 577 Antioxidant activity in Lingonberries (Vaccinium vitis-idaea L.) and its

- inhibitory effect on activator protein-1, nuclear factor-κB, and
  mitogen-activated Protein kinases activation. *J. Agric. Food Chem.* 2005, 53,
  3156–3166.
- (35) Dai, R.; Chen, R.; Li, H. Cross-talk between PI3K/Akt and MEK/ERK
  pathways mediates endoplasmic reticulum stress-induced cell cycle progression
  and cell death in human hepatocellular carcinoma cells. *Int. J. Oncol.* 2009, *34*,
  1749-1757.
- (36) Liu, H.; Xiao, Y.; Xiong, C.; Wei, A.; Ruan J. Apoptosis induced by a new
  flavonoid in human hepatoma HepG2 cells involves reactive oxygen
  species-mediated mitochondrial dysfunction and MAPK activation. *Eur. J.*
- 588 *Pharmacol.* **2011**, *654*, 209–216.
- 589 (37) Zhou, P.; Gross, S.; Liu, J. H.; Yu, B. Y.; Feng, L. L.; Nolta, J.; Sharma, V.;
- 590 Piwnica-Worms, D.; and Qiu, S. X. Flavokawain B, the hepatotoxic constituent
- 591 from kava root, induces GSH-sensitive oxidative stress through modulation of
- 592 IKK/NF-κB and MAPK signaling Pathways. *FASEB J.* **2010**, *24*, 4722-4732.
- (38) Ogryzko, V.V.; Wong, P.; Howard, B.H. WAF1 retards S-phase progression
  primarily by inhibition of cyclin-dependent kinases. *Mol Cell Biol.* 1997, 17,
  4877-4882.
- 596 (39) Hsu, J. D.; Kao, S.H.; Ou, T. T.; Chen, Y. J.; Li, Y. J.; Wang, C. J. Gallic acid
- 597 induces G2/M phase arrest of breast cancer cell MCF-7 through stabilization of

- $p27^{Kip1}$  attributed to disruption of  $p27^{Kip1}/Skp2$  complex. J. Agric. Food Chem.
- , *59*, 1996–2003.